Compressed-liquid densities of two highly polar + non-polar binary systems ☆

Stephanie L. Outcalt *, Arno Laesecke

National Institute of Standards and Technology, Material Measurement Laboratory, Thermophysical Properties Division, 325 Broadway, Boulder, CO 80305-3337, USA

ABSTRACT

The binary systems ethanol + 2,2,4-trimethylpentane and 2-butanol + 2,2,4-trimethylpentane were studied as models for blends of gasoline with biofuels. Their densities were measured with a vibrating-tube densimeter at compressed-liquid states of three compositions of each of the binary systems. The temperature and pressure ranges of the measured data are from 270 K to 470 K, and 0.5 MPa to 50 MPa. There are no compressed-liquid density data for the binary system ethanol + 2,2,4-trimethylpentane in the literature, thus data reported here are compared to literature data at atmospheric pressure in order to establish their quality. No literature data for the system 2-butanol + 2,2,4-trimethylpentane were found, thus data reported here fill a void and help to further the understanding of molecular interactions in binary systems of a polar and a non-polar compound.

Published by Elsevier B.V.

1. Introduction

Governments in countries around the world are increasingly mandating the use of biofuels. In 1988, Denver, Colorado was the first in the United States to mandate the use of ethanol oxygenated fuel during winter months in order to reduce carbon dioxide emissions [1]. Every year from November to March, the gasoline sold in that metropolitan area is blended with 10% ethanol by volume, some of which is provided from the waste streams of a nearby brewery. In April of 2009, Directive 2009/28/EC of the European Parliament included the goal of a minimum of 10% use of biofuels or other renewable energy in the transport sector by 2020. The US Renewable Fuel Standard calls for 136 billion liters of biofuel blended into the US domestic auto and truck fuel supply by early 2022.

In spite of the widespread adoption of the use of biofuels, there is still much to learn about the thermophysical properties of these complex mixtures. Knowledge of such properties is necessary for many purposes such as the efficient design of engines and determining if the existing infrastructure will be adequate for large-scale distribution

of the fuels. Biofuels often include blends of highly polar compounds with non-polar hydrocarbons. The interactions of the dissimilar molecules in these types of blends are difficult to model accurately, because they are strongly non-ideal. Measurements of such systems are more difficult than those of nonpolar compounds and their mixtures because of the physical attributes of polar compounds such as their hygroscopicity. As a result, accurate literature data for the development of non-ideal property models are sparse or non-existent. The systems investigated in this work are examples for both.

In an effort to better understand how polar + non-polar interactions affect the thermophysical properties of mixtures, the primary goal of the work presented here was to select binary systems whose pure fluid components are representative of those found in biofuel blends and then to measure their compressed-liquid densities over a wide range of temperature and pressure. Measurements such as those presented here help to reveal the non-ideal behavior of the mixtures. The binary mixtures chosen for this study were ethanol + 2,2,4-trimethylpentane and 2-butanol + 2,2,4-trimethylpentane. They are considered as model mixtures for blends of gasoline with biofuels where 2,2,4-trimethylpentane represents gasoline while ethanol and 2-butanol are first- and second-generation biofuels derived from biomass. Measurements of compressed-liquid densities were carried out for three compositions of each of the binary mixtures with nominal mole fractions of 2,2,4-trimethylpentane of 0.25, 0.5, and 0.75 over the temperature range from 270 K to 470 K with pressures from 0.5 MPa to 50 MPa.

---

2. Sample liquids

Each of the three pure fluids used to prepare the mixtures studied in this work was obtained from a commercial source. The 2-butanol (CAS number 78-92-2) had a stated minimum purity of 99.5% by mole. Because of its hygroscopicity, activated molecular sieve type 5A, grade 521, with an effective pore size of 0.5 nm was added to the sample bottle to keep the 2-butanol dry. Prior to mixture preparation, the water content was just at the detection limit of approximately 20 ppm as measured by Karl Fischer coulombic titrimetry. The 2,2,4-trimethylpentane (CAS number, 540-84-1, here after referred to as iso-octane) had a stated molar purity of 99.8% and the ethanol (CAS number 78-92-2) one of 99.5%. Both were used without further purification.

The binary mixtures of ethanol + iso-octane and 2-butanol + iso-octane measured in this work were prepared gravimetrically in cleaned and dried glass bottles. The balance used in the mixture preparation had a manufacturer's stated repeatability of 0.3 g. Prior to measurements, each of the samples was transferred to a clean, dry, stainless steel bottle. The samples were then subjected to a series of being frozen with liquid nitrogen, evacuating the space above the frozen sample, and thawing the sample. This was done in order to remove air and/or any other volatile impurities from the sample, and did not affect the mixture composition.

3. Experimental

The densities of the compressed test liquids were measured with the automated densimeter that was used in our previous studies [2–9]. Central to the apparatus is a commercial vibrating-tube densimeter.

Several physical and procedural improvements have been implemented beyond that of the commercial instrument operated in a stand-alone mode in order to minimize the uncertainty in the measurements. Some of these improvements include more accurate measurements of temperature and pressure, better temperature control, complete automation of the instrument control and data acquisition, and a comprehensive assessment of uncertainty. The temperature range of the instrument is 270 K to 470 K with pressures up to 50 MPa. The instrument was calibrated with propane and toluene over the entire temperature and pressure range. Further details of the calibration procedure can be found in the paper by Outcalt and McLinden [2]. The overall combined expanded uncertainty ($k = 2$) in density is 1.5 kg·m^{-3}, corresponding to a relative uncertainty in density of 0.19% to 0.30%. This uncertainty is far greater than the 0.81 kg·m^{-3} reported for measurements of pure fluids with this instrument. This is because it includes all of the uncertainties associated with pure fluids plus the uncertainty in the composition of the mixture.

4. Results and discussion

Tables 1 to 3 list the measured density values of three compositions of compressed-liquid ethanol + iso-octane from 270 K to 470 K to pressures of 50 MPa. A total of 375 data points are reported for this system. Tables 4 through 6 list the measured density values of the three compositions of compressed-liquid 2-butanol + iso-octane from 270 K to 470 K to pressures of 50 MPa. A total of 357 data points are reported for this system. No measurements of the mixture with 25.1% 2-butanol were conducted at 470 K. This is due to difficulties during the course of the measurements which completely depleted the supply of the standard mixture prior to measuring the final isotherm. For all

Table 1

Compressed-liquid densities of the binary system ethanol + iso-octane (25.1/74.9 mol%) measured in the high pressure vibrating-tube densimeter along isotherms from 270 K to 470 K.

270 K		290 K		310 K		330 K		350 K		370 K	
Pressure p	Density ρ	Pressure p	Density ρ	Pressure p	Density ρ	Pressure p	Density ρ	Pressure p	Density ρ	Pressure p	Density ρ
MPa	kg·m^{-3}	MPa	kg·m^{-3}	MPa	kg·m^{-3}	MPa	kg·m^{-3}	MPa	kg·m^{-3}	MPa	kg·m^{-3}
50.00	755.0	49.97	742.7	50.03	730.5	50.01	717.9	50.02	705.0	50.02	691.9
40.00	749.3	39.99	736.4	39.99	723.7	40.00	710.5	40.01	696.9	40.00	683.1
29.99	743.1	30.01	729.6	30.01	716.3	30.00	702.3	30.00	687.8	30.00	673.1
20.01	736.4	20.00	722.2	20.00	708.0	20.00	693.1	20.00	677.6	20.01	661.7
10.00	729.0	10.00	713.9	10.00	698.8	10.00	682.6	10.01	665.7	10.01	648.0
5.00	725.0	5.00	709.4	5.00	693.6	5.00	676.7	5.00	658.8	4.99	639.9
4.00	724.2	4.00	708.5	4.00	692.6	4.00	675.4	3.99	657.3	4.00	638.2
3.00	723.4	2.99	707.5	3.00	691.4	3.00	674.2	3.00	655.8	3.00	636.3
2.00	722.5	2.00	706.5	2.01	690.3	2.00	672.8	2.00	654.2	2.00	634.5
0.99	721.6	1.00	705.5	1.00	689.2	0.99	671.5	1.00	652.7	1.00	632.5
0.50	721.2	0.49	705.0	0.50	688.6	0.50	670.8	0.50	651.8	0.50	631.5

390 K		410 K		430 K		450 K		470 K	
Pressure p	Density ρ	Pressure p	Density ρ	Pressure p	Density ρ	Pressure p	Density ρ	Pressure p	Density ρ
MPa	kg·m^{-3}	MPa	kg·m^{-3}	MPa	kg·m^{-3}	MPa	kg·m^{-3}	MPa	kg·m^{-3}
50.01	679.3	50.01	666.5	50.02	654.0	50.02	641.4	50.01	628.6
40.00	669.6	40.00	656.0	40.00	642.5	40.00	628.9	40.00	615.1
30.00	658.6	30.00	643.8	30.00	629.1	30.00	614.2	30.00	598.8
20.00	645.7	20.00	629.3	20.00	612.7	20.00	595.7	20.01	578.0
10.00	629.9	10.00	610.9	10.00	591.2	10.00	570.3	10.00	548.0
5.00	620.3	5.00	599.2	5.01	576.7	5.01	552.1	5.00	524.5
4.00	618.1	4.00	596.5	4.49	575.0	4.50	549.9	4.50	521.4
3.00	615.9	3.00	593.7	3.99	573.2	4.00	547.5	4.00	518.1
2.00	613.5	2.00	590.8	3.51	571.5	3.51	545.2	3.50	514.6
0.99	611.1	1.00	587.7	3.00	569.6	3.00	542.4	3.00	510.9
0.50	609.9	0.50	586.0	2.50	567.7	2.50	539.7	2.50	506.8
				2.01	565.8	1.99	536.8	2.00	502.3
				1.50	563.7	1.50	533.9		
				1.00	561.5				

The combined expanded uncertainties U_c are $U_c(T) = 30$ mK, $U_c(p) = 10$ kPa, $U_c(\rho) = 1.5$ kg·m^{-3} (level of confidence = 0.95).

Table 2
Compressed-liquid densities of ethanol + iso-octane (50.0/50.0 mol%) measured in the high pressure vibrating-tube densimeter along isotherms from 270 K to 470 K.

270 K		290 K		310 K		330 K		350 K		370 K	
Pressure p	Density ρ	Pressure p	Density ρ	Pressure p	Density ρ	Pressure p	Density ρ	Pressure p	Density ρ	Pressure p	Density ρ
MPa	kg·m^{-3}	MPa	kg·m^{-3}	MPa	kg·m^{-3}	MPa	kg·m^{-3}	MPa	kg·m^{-3}	MPa	kg·m^{-3}
49.98	769.9	49.98	756.3	50.00	743.9	49.99	730.3	50.01	716.6	50.02	702.7
39.99	764.1	40.01	750.0	40.00	737.1	40.01	722.8	40.00	708.5	40.00	693.8
30.00	757.8	30.00	743.2	30.00	729.6	30.00	714.6	30.01	699.4	30.00	683.7
19.99	751.0	20.01	735.7	20.01	721.4	20.00	705.4	20.00	689.2	20.00	672.2
9.99	743.6	10.00	727.5	10.00	712.1	10.01	695.0	10.00	677.3	10.01	658.5
4.99	739.6	5.00	723.0	5.00	707.0	5.00	689.1	5.01	670.5	4.99	650.5
4.00	738.8	4.00	722.0	4.00	705.9	4.01	687.8	4.00	669.0	4.00	648.7
3.00	738.0	3.00	721.1	3.00	704.8	3.00	686.6	3.00	667.5	3.01	646.9
2.00	737.1	2.00	720.1	2.00	703.7	1.99	685.3	2.00	666.0	2.01	645.1
0.99	736.2	0.99	719.1	1.00	702.6	1.00	683.9	1.00	664.4	1.00	643.2
0.50	735.8	0.50	718.6	0.50	702.0	0.50	683.3	0.50	663.6	0.50	642.2

390 K		410 K		430 K		450 K		470 K	
Pressure p	Density ρ	Pressure p	Density ρ	Pressure p	Density ρ	Pressure p	Density ρ	Pressure p	Density ρ
MPa	kg·m^{-3}	MPa	kg·m^{-3}	MPa	kg·m^{-3}	MPa	kg·m^{-3}	MPa	kg·m^{-3}
50.01	688.5	50.01	674.2	50.00	659.5	49.99	644.8	50.00	630.2
39.99	678.7	40.00	663.4	39.99	647.6	40.00	631.7	40.00	615.9
30.01	667.6	30.01	651.0	29.99	633.7	29.99	616.1	30.01	598.4
20.00	654.6	20.00	636.1	20.00	616.7	20.01	596.6	20.00	575.8
10.01	638.6	10.00	617.3	10.01	594.2	10.00	569.2	9.99	542.1
5.00	628.9	5.00	605.3	5.00	579.0	5.00	549.1	5.01	514.3
4.00	626.7	4.00	602.6	4.50	577.2	4.50	546.7	4.50	510.4
2.99	624.5	3.00	599.7	4.00	575.4	4.00	544.1	4.00	506.2
2.00	622.2	2.00	596.7	3.50	573.5	3.49	541.3	3.50	501.6
0.99	619.8	1.00	593.6	2.99	571.5	3.01	538.5	2.99	496.5
0.50	618.6			2.50	569.5	2.49	535.3		
				2.00	567.4	2.00	532.1		
				1.50	565.2				

The combined expanded uncertainties U_c are $U_c(T) = 30$ mK, $U_c(p) = 10$ kPa, $U_c(\rho) = 1.5$ kg·m^{-3} (level of confidence = 0.95).

of the samples, when no densities at lower pressures are reported, it is because stable readings were not achieved. These instances occur only at temperatures of 410 K and above and are most likely due to sample evaporation when approaching the vapor pressures at those temperatures.

4.1. Mixture model as baseline for comparisons

To provide a benchmark for comparisons, a model explicit in the Helmholtz free energy was adjusted to the present density data for the system ethanol + iso-octane. The model was originally formulated for mixtures of fluorinated and chlorinated hydrocarbons [10]. The properties of ethanol were entered into the mixture model from a newly developed fundamental equation [11]. A preliminary NIST formulation for the Helmholtz free energy of iso-octane was used that is presently being refined to greater accuracy by taking into account additional recent experimental data. The adjustment to the present density data was based on the excess function optimized for difluoromethane (R32) + 1,1,1,2-tetrafluoroethane (R134a), and the parameter F_{ij} in the mixture model [10] was also set to unity.

Figs. 1 to 3 show the deviations between the experimental compressed-liquid density data and those calculated with the Helmholtz free energy mixture model as a function of pressure at ethanol mole fractions of 25.1%, 50.0%, and 75.0%, respectively. At 25 mol% ethanol (Fig. 1), the model represents the majority of the experimental data within their estimated expanded uncertainty of 0.3%. The spread of the deviations indicates that the model can be improved further to represent the temperature dependence of the data. The spreads of the deviations increase with increased ethanol content but not in a linear fashion. The deviations for the mixture with a mole

fraction of 50% ethanol range from −1.1% to 0.31%, while the data of the mixture with a mole fraction of 75% ethanol are represented from −0.4% to 0.74%. The origins of these deviations will be discussed in a later section.

A similar model explicit in the Helmholtz free energy was not formulated for the binary system 2-butanol + iso-octane, because a suitable equation of state is not yet available for 2-butanol. In our previous work [7], we reported density measurements of compressed liquid 2-butanol that were represented by a Tait-type equation of state. This equation relates pressure, density, and temperature, but unlike a Helmholtz free energy equation, it cannot predict other thermophysical properties.

4.2. Comparisons with literature data for ethanol + iso-octane at atmospheric pressure

A survey of the literature for density data for the two binary mixtures revealed no density data for the 2-butanol + iso-octane system and only ambient pressure data for ethanol + iso-octane. Table 7 lists the sources of data and their temperature ranges for the ethanol + iso-octane mixture [2–20]. From the table, it can be seen that the data available in the literature cover a rather limited temperature range with the most comprehensive set being that of Gonzalez-Olmos et al. [20].

Figs. 4 and 5 illustrate the deviations of the literature data for the sources compiled in Table 7. They are compared to a baseline of the preliminary Helmholtz free energy model for the ethanol + iso-octane mixture as a function of temperature and mole fraction of ethanol, respectively. The stated uncertainty of most of the data shown is less than or equal to 0.3 kg·m^{-3}, which corresponds to relative

Table 3
Compressed-liquid densities of ethanol + iso-octane (75.0/25.0 mol%) measured in the high pressure vibrating-tube densimeter along isotherms from 270 K to 470 K.

270 K		290 K		310 K		330 K		350 K		370 K	
Pressure p	Density ρ	Pressure p	Density ρ	Pressure p	Density ρ	Pressure p	Density ρ	Pressure p	Density ρ	Pressure p	Density ρ
MPa	kg·m^{-3}	MPa	kg·m^{-3}	MPa	kg·m^{-3}	MPa	kg·m^{-3}	MPa	kg·m^{-3}	MPa	kg·m^{-3}
50.01	793.9	50.00	780.1	50.02	767.6	50.01	753.7	50.02	739.8	50.01	725.4
39.99	788.1	40.00	773.8	39.99	760.8	40.00	746.3	39.99	731.8	40.00	716.7
29.99	781.9	30.00	767.1	30.00	753.5	30.00	738.3	29.99	723.0	30.00	706.9
19.99	775.2	20.00	759.8	19.99	745.5	20.01	729.5	20.00	713.1	20.00	695.9
10.00	768.0	10.00	751.7	9.99	736.5	10.00	719.4	10.00	701.8	9.99	682.8
4.99	764.1	5.00	747.4	4.99	731.6	4.99	713.8	5.00	695.3	4.99	675.3
4.00	763.3	3.99	746.4	4.00	730.6	4.00	712.7	4.00	694.0	4.00	673.6
3.00	762.5	3.00	745.5	2.99	729.6	3.00	711.5	2.99	692.5	2.99	671.9
1.99	761.6	2.00	744.6	2.00	728.5	2.00	710.2	1.99	691.1	2.00	670.2
1.00	760.8	1.00	743.7	1.00	727.4	0.99	709.0	0.99	689.7	0.99	668.5
0.49	760.4	0.50	743.2	0.49	726.9	0.50	708.4	0.49	688.9	0.50	667.6

390 K		410 K		430 K		450 K		470 K	
Pressure p	Density ρ	Pressure p	Density ρ	Pressure p	Density ρ	Pressure p	Density ρ	Pressure p	Density ρ
MPa	kg·m^{-3}	MPa	kg·m^{-3}	MPa	kg·m^{-3}	MPa	kg·m^{-3}	MPa	kg·m^{-3}
50.02	710.5	50.01	695.0	50.02	678.8	50.01	662.0	50.02	645.1
40.00	700.9	39.99	684.3	40.00	667.0	39.99	648.8	40.00	630.3
29.99	690.1	29.99	672.2	30.00	653.2	30.00	633.2	29.99	612.4
20.00	677.5	20.00	657.8	19.99	636.5	20.00	613.6	20.00	589.2
10.00	662.3	10.00	639.7	10.00	614.6	10.00	586.4	10.00	554.5
5.00	653.2	4.99	628.5	5.00	600.1	4.99	566.7	5.00	525.3
3.99	651.2	4.49	627.2	4.50	598.5	4.50	564.3	4.50	521.2
3.00	649.2	3.99	625.9	3.99	596.7	3.99	561.8	4.00	516.9
2.00	647.0	3.50	624.6	3.50	595.0	3.49	559.1	3.50	511.9
1.00	644.8	2.99	623.3	2.99	593.1	2.99	556.4	3.00	506.5
0.50	643.7	2.49	621.9	2.50	591.2	2.50	553.4		
		1.99	620.5	1.99	589.3	1.99	550.2		
		1.50	619.1	1.49	587.2				
		1.00	617.6						

The combined expanded uncertainties U_c are $U_c(T) = 30$ mK, $U_c(p) = 10$ kPa, $U_c(\rho) = 1.5$ kg·m^{-3} (level of confidence = 0.95).

uncertainties of approximately 0.05%. The figures show that the preliminary Helmholtz free energy model does not represent the data within their reported uncertainty, nor is there particularly good agreement between the various literature data sets. The deviations as a function of temperature in Fig. 4 are consistent with the temperature trend of the deviations between the present data and the preliminary model. Systematic deviations as a function of mixture composition can be seen in Fig. 5. Most of the deviations are negative with minima at ethanol mole fractions between 0.5 and 0.6. These deviations will be revisited in a later section.

4.3. Molecular characteristics

In order to understand and interpret the results of the measurements presented herein it is helpful to have some understanding of the typical behavior of polar versus non-polar pure fluids. As an example, Fig. 6 shows the vapor pressures of ethanol, 2-butanol, and iso-octane as a function of temperature in the range of the present measurements 270 K to 470 K. The vapor pressures were calculated with the correlations implemented in REFPROP [21] (ethanol [11] and iso-octane [22]) and DIPPR [23] (2-butanol). At low temperatures, the vapor pressure of ethanol is lower than that of iso-octane. But at approximately 280 K, both compounds have the same vapor pressure and that of ethanol exceeds that of iso-octane at higher temperatures. A similar phenomenon occurs with the vapor pressure of 2-butanol, except that the temperature of equal vapor pressure with iso-octane is increased to approximately 375 K.

The stronger temperature dependence of properties such as density and viscosity is a typical characteristic of polar compounds [24]. It arises from electrostatic attractions due to the non-uniform charge

distributions in such molecules [25,26]. In alcohols, the electrostatic attractions are so strong that the molecules associate via hydrogen bonds thus forming the particular structures of their solid and liquid phases as well as promoting clusters in their gas phases [27,28]. To illustrate this difference between the two polar alcohols and the non-polar iso-octane, the sizes, shapes, and charge distributions of these molecules were calculated from first principles with the hybrid density functional model B3LYP and 6-311 + G** polarization basis sets. Surfaces of constant electron density at 0.002 electrons·a.u.$^{-3}$, with 1 a.u. = 5.292 nm being the Bohr radius of hydrogen, were also computed. Electron density is a measure of the probability of an electron being present at a certain location, and the isodensity surfaces shown in Fig. 7 contain approximately 99% of a molecule. Isoelectron density surfaces convey more realistic impressions than models of fused hard spheres, because they are smooth and because they represent molecules as soft and deformable entities instead of rigid assemblies of spheres. This is important to understand the roles of attractive and repulsive forces in molecular interactions as well as that of polarizability, which characterizes the stiffness of the electron cloud against an electric field. An additional and unique advantage of computer graphics of molecular structures is that charge distributions across molecules can be visualized. In Fig. 7, the electrostatic potential is color-mapped onto the isoelectron density surfaces with a scale ranging from red (negative charge) to blue (positive charge). This color-mapping makes the non-uniform charge distributions visible and thus facilitates the understanding of the contributions of electrostatic forces to intermolecular interactions. The common color scale for the three molecules in Fig. 7 is that for the electrostatic potential of ethanol with a range from -181 kJ·mol^{-1} to 216 kJ·mol^{-1}. The dotted parts of the isosurfaces signify areas that are inaccessible if a

Table 4
Compressed-liquid densities of 2-butanol + iso-octane (25.1/74.9 mol%) measured in the high pressure vibrating-tube densimeter along isotherms from 270 K to 450 K.

270 K		290 K		310 K		330 K		350 K		370 K	
Pressure p	Density ρ	Pressure p	Density ρ	Pressure p	Density ρ	Pressure p	Density ρ	Pressure p	Density ρ	Pressure p	Density ρ
MPa	kg·m^{-3}	MPa	kg·m^{-3}	MPa	kg·m^{-3}	MPa	kg·m^{-3}	MPa	kg·m^{-3}	MPa	kg·m^{-3}
50.02	761.2	49.95	748.1	50.02	735.2	49.99	722.1	50.00	709.1	50.01	696.0
40.00	755.5	40.00	741.9	40.00	728.5	40.00	714.8	40.00	701.1	40.01	687.2
30.00	749.4	29.99	735.2	30.00	721.1	30.00	706.7	30.00	692.2	30.01	677.4
20.00	742.7	19.99	727.8	20.01	713.0	20.00	697.7	20.00	682.1	19.99	666.2
10.00	735.5	10.00	719.7	10.01	703.9	10.00	687.4	10.01	670.4	10.01	652.8
5.00	731.6	5.01	715.2	5.00	698.8	5.00	681.6	5.00	663.7	4.99	644.9
4.00	730.8	3.99	714.2	4.01	697.8	4.00	680.4	4.00	662.2	4.01	643.3
2.99	730.0	3.00	713.3	3.00	696.7	3.01	679.1	3.00	660.8	3.00	641.5
1.99	729.2	2.00	712.4	2.00	695.6	2.00	677.8	2.00	659.3	2.00	639.7
1.00	728.3	1.00	711.4	1.00	694.5	1.00	676.5	1.00	657.8	1.01	637.9
0.50	727.9	0.51	710.9	0.50	693.9	0.50	675.9	0.50	657.0	0.49	636.9

390 K		410 K		430 K		450 K	
Pressure p	Density ρ	Pressure p	Density ρ	Pressure p	Density ρ	Pressure p	Density ρ
MPa	kg·m^{-3}	MPa	kg·m^{-3}	MPa	kg·m^{-3}	MPa	kg·m^{-3}
49.99	682.9	49.99	670.0	50.00	657.3	50.00	644.9
40.01	673.4	40.00	659.7	40.00	646.2	40.01	632.8
30.00	662.6	30.00	647.8	30.00	633.2	29.99	618.5
20.00	650.0	20.00	633.8	20.00	617.4	20.00	600.9
10.00	634.7	10.00	616.1	10.00	597.0	10.00	577.1
5.01	625.4	5.00	605.0	5.01	583.6	5.00	560.6
4.00	623.4	4.00	602.5	4.00	580.5	4.01	556.7
3.01	621.2	3.01	599.9	3.00	577.2	3.00	552.4
2.00	619.0	2.00	597.2	2.00	573.7	2.00	547.7
1.00	616.8	1.01	594.3	1.00	570.0	1.00	542.6
0.51	615.6	0.50	592.8	0.50	568.0		

The combined expanded uncertainties U_c are $U_c(T) = 30$ mK, $U_c(p) = 10$ kPa, $U_c(\rho) = 1.5$ kg·m^{-3} (level of confidence = 0.95).

Table 5
Compressed-liquid densities of 2-butanol + iso-octane (50/50 mol%) measured in the high pressure vibrating-tube densimeter along isotherms from 270 K to 470 K.

270 K		290 K		310 K		330 K		350 K		370 K	
Pressure p	Density ρ	Pressure p	Density ρ	Pressure p	Density ρ	Pressure p	Density ρ	Pressure p	Density ρ	Pressure p	Density ρ
MPa	kg·m^{-3}	MPa	kg·m^{-3}	MPa	kg·m^{-3}	MPa	kg·m^{-3}	MPa	kg·m^{-3}	MPa	kg·m^{-3}
50.01	783.9	50.00	770.7	50.03	757.7	50.01	743.4	50.01	729.5	50.02	715.4
40.00	778.3	40.00	764.6	40.00	751.0	40.00	736.2	40.00	721.6	40.00	706.7
30.00	772.4	30.00	758.0	30.00	743.8	30.00	728.2	30.00	712.9	30.00	697.1
20.01	766.0	20.00	750.9	20.01	735.8	20.00	719.5	20.00	703.1	20.00	686.1
10.00	759.0	10.00	743.1	10.00	727.0	10.00	709.5	10.00	691.8	10.00	673.1
5.01	755.2	5.00	738.8	5.00	722.1	5.01	703.9	5.00	685.3	5.00	665.6
4.00	754.5	4.01	737.9	4.00	721.1	4.00	702.7	4.00	684.0	4.01	663.9
3.00	753.7	3.00	737.0	3.01	720.0	3.00	701.6	3.00	682.6	3.00	662.3
2.00	752.9	2.00	736.1	2.01	719.0	2.00	700.3	2.00	681.1	2.01	660.6
1.00	752.0	1.00	735.2	1.01	717.9	1.00	699.1	1.01	679.7	1.01	658.8
0.51	751.6	0.51	734.7	0.50	717.4	0.50	698.5	0.49	678.9	0.50	657.9

390 K		410 K		430 K		450 K		470 K	
Pressure p	Density ρ	Pressure p	Density ρ	Pressure p	Density ρ	Pressure p	Density ρ	Pressure p	Density ρ
MPa	kg·m^{-3}	MPa	kg·m^{-3}	MPa	kg·m^{-3}	MPa	kg·m^{-3}	MPa	kg·m^{-3}
50.00	701.1	50.00	687.0	50.02	672.9	50.01	658.7	50.03	645.0
40.00	691.7	40.00	676.7	40.01	661.7	40.00	646.5	40.01	631.6
30.00	681.0	30.00	664.9	30.00	648.7	30.01	632.0	30.00	615.6
20.00	668.7	19.99	650.9	20.00	632.9	20.00	614.1	20.00	595.4
10.00	653.7	10.01	633.6	10.00	612.5	10.00	590.1	9.99	566.9
5.00	644.7	5.00	622.7	5.00	599.3	5.00	573.5	5.01	545.7
4.00	642.8	4.00	620.3	4.00	596.2	4.00	569.5	4.00	540.2
3.00	640.7	3.00	617.8	3.00	593.0	3.00	565.2	3.01	534.1
2.01	638.6	2.00	615.2	2.01	589.6	2.00	560.6		
1.00	636.5	1.01	612.4	1.00	586.0	1.01	555.4		
0.51	635.4	0.50	611.0						

The combined expanded uncertainties U_c are $U_c(T) = 30$ mK, $U_c(p) = 10$ kPa, $U_c(\rho) = 1.5$ kg·m^{-3} (level of confidence = 0.95).

Table 6
Compressed-liquid densities of 2-butanol + iso-octane (75/25 mol%) measured in the high pressure vibrating-tube densimeter along isotherms from 270 K to 470 K.

270 K		290 K		310 K		330 K		350 K		370 K	
Pressure p	Density ρ	Pressure p	Density ρ	Pressure p	Density ρ	Pressure p	Density ρ	Pressure p	Density ρ	Pressure p	Density ρ
MPa	kg·m^{-3}	MPa	kg·m^{-3}	MPa	kg·m^{-3}	MPa	kg·m^{-3}	MPa	kg·m^{-3}	MPa	kg·m^{-3}
49.98	813.3	49.98	800.1	50.00	786.5	50.01	772.0	50.03	757.3	50.02	742.1
40.01	807.9	40.01	794.2	40.00	780.1	40.00	765.0	40.00	749.7	40.00	733.8
30.00	802.2	30.00	788.0	30.00	773.3	30.00	757.5	30.00	741.3	30.00	724.5
20.00	796.1	20.00	781.3	20.00	765.8	20.00	749.2	20.00	732.0	20.01	714.0
10.00	789.5	10.00	773.9	10.00	757.5	10.00	739.8	10.01	721.4	10.00	701.8
5.00	786.0	5.00	769.9	5.00	753.0	5.01	734.7	5.01	715.4	5.00	694.8
4.00	785.2	3.99	769.1	3.99	752.0	4.00	733.6	4.00	714.1	4.00	693.3
3.00	784.5	3.00	768.2	3.00	751.1	3.00	732.5	3.00	712.8	3.00	691.8
2.01	783.8	2.00	767.4	2.00	750.1	1.99	731.3	2.00	711.5	2.00	690.2
1.00	783.0	1.00	766.6	1.00	749.1	1.01	730.2	1.00	710.2	1.00	688.6
0.50	782.6	0.50	766.1	0.50	748.6	0.50	729.6	0.50	709.5	0.50	687.8

390 K		410 K		430 K		450 K		470 K	
Pressure p	Density ρ	Pressure p	Density ρ	Pressure p	Density ρ	Pressure p	Density ρ	Pressure p	Density ρ
MPa	kg·m^{-3}	MPa	kg·m^{-3}	MPa	kg·m^{-3}	MPa	kg·m^{-3}	MPa	kg·m^{-3}
50.03	726.6	50.00	710.8	50.03	695.0	50.01	679.3	50.00	663.9
40.01	717.4	40.00	700.7	40.00	683.9	40.00	667.1	40.00	650.4
30.00	707.1	30.00	689.2	30.01	671.1	30.00	652.8	30.00	634.4
20.00	695.3	20.00	675.8	19.99	655.7	20.00	635.2	20.01	614.4
10.01	681.2	10.00	659.3	10.01	636.3	10.00	612.1	10.01	586.5
5.00	672.9	5.00	649.3	5.01	623.9	8.00	606.3	9.01	582.9
4.00	671.1	4.00	647.0	4.00	621.1	6.00	599.9	8.00	579.1
3.00	669.2	3.00	644.7	3.00	618.1	5.00	596.4	7.00	575.1
2.00	667.3	2.00	642.4	2.00	615.0	4.00	592.8	6.00	570.7
1.00	665.3	1.00	639.9	1.01	611.8	2.99	588.8	4.99	566.0
0.50	664.3	0.50	638.6			2.00	584.6	3.00	555.3
						1.00	580.0		

The combined expanded uncertainties U_c are $U_c(T) = 30$ mK, $U_c(p) = 10$ kPa, $U_c(\rho) = 1.5$ kg·m^{-3} (level of confidence = 0.95).

sphere of radius 0.1 nm centered on a line normal to the isosurface and touching a point in the middle of the region, impinges on any other regions of the isosurface [29]. These inaccessible parts are indicative of the geometry-dependent void volume between molecules of the same species which contributes to their packing density. The relative contribution of the void volumes to the system density becomes more prominent with increasing pressure and decreasing temperature.
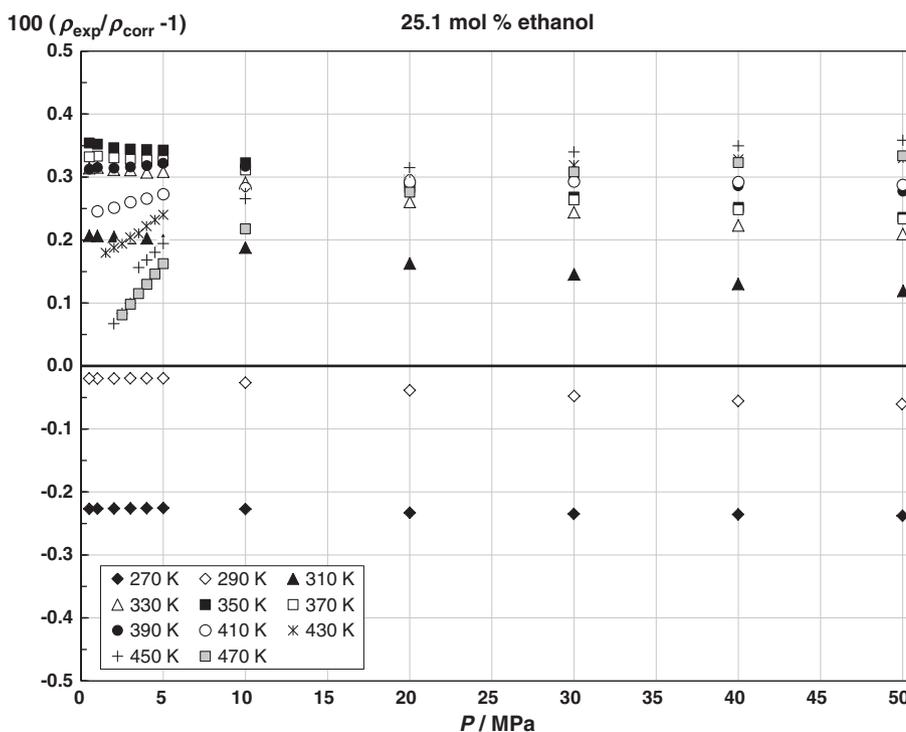
Fig. 1. Deviations between compressed-liquid density data for the mixture with 25 mol% ethanol measured in this work and those calculated with the preliminary Helmholtz free energy mixture model as a function of pressure.
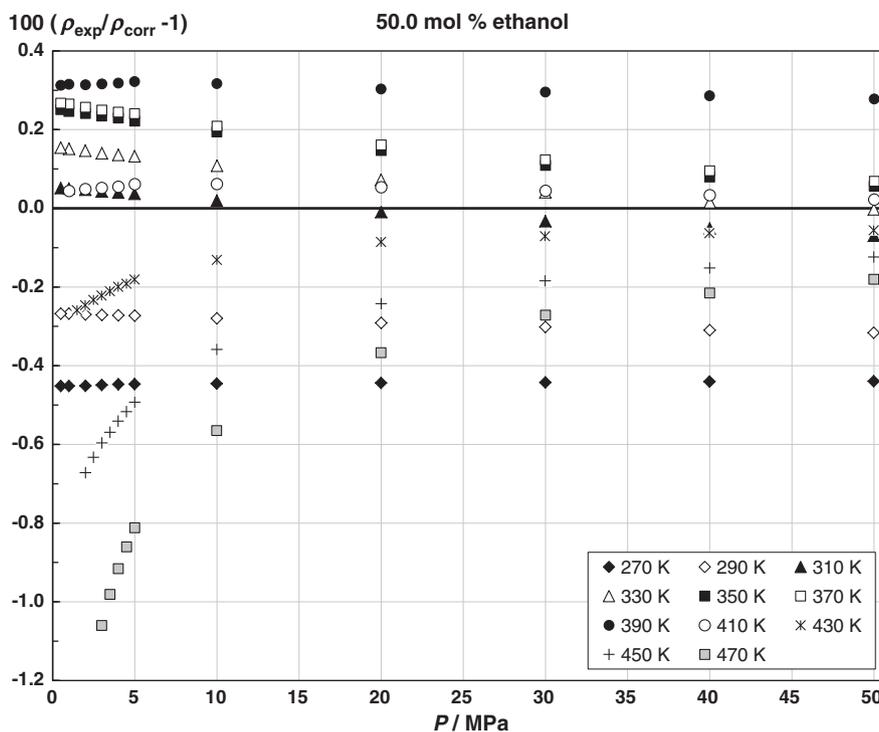
Fig. 2. Deviations of compressed-liquid density data for the mixture with 50 mol% ethanol measured in this work and those calculated with the preliminary Helmholtz free energy mixture model as a function of pressure.

Numerical results of the first principle calculations are listed in Table 8. The ovality O is obtained as a ratio between surface area A and volume V according to

$$O = A / \left(4\pi \left(\frac{3V}{4} \pi \right)^{2/3} \right).$$

For spheres, $O = 1$. The greater O, the more cylindrical is a molecule.

The polar surface area (PSA) is defined as the area due to oxygen and the hydrogens attached to oxygen [30]. It is noteworthy that the PSA in ethanol is greater than that in 2-butanol. This reflects the higher polarity of ethanol and a more negative partial charge of its OH-group. The molecular characteristics explored in this section are
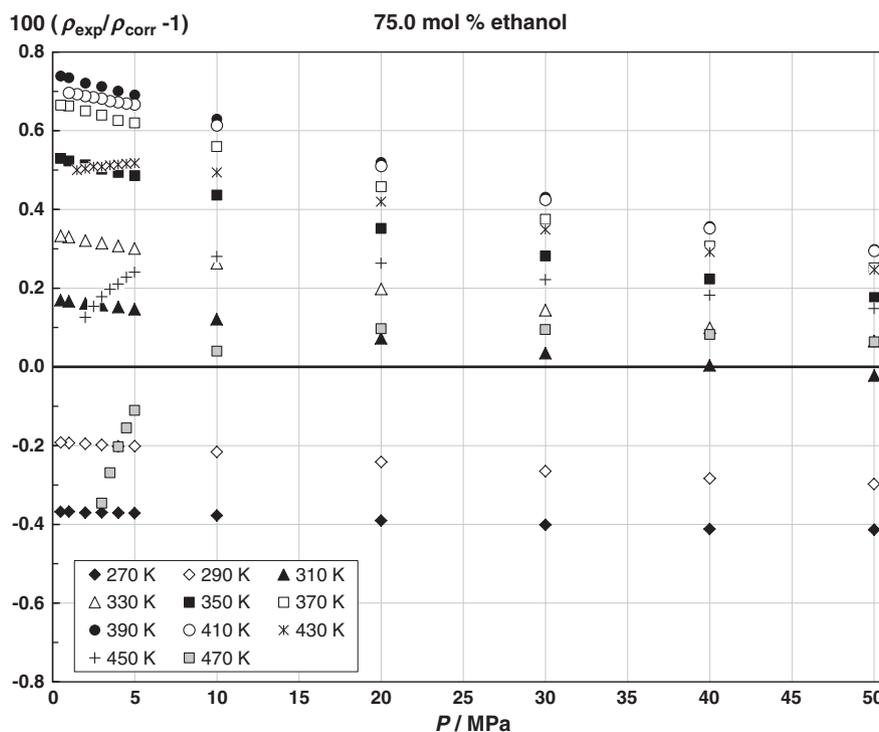
Fig. 3. Deviations of compressed-liquid density data for the mixture with 75 mol% ethanol measured in this work and those calculated with the preliminary Helmholtz free energy mixture model as a function of pressure.

Table 7
Literature sources of density data for mixtures of ethanol + iso-octane.

Authors	Year	Measured temperatures [K]
Gonzalez-Olmos et al.	2010	288.15, 298.15, 323.15
Kim et al.	2009	303.15
In and Park	2008	298.15
Hwang et al.	2007	293.15
Chen and Tu	2006	288.15, 298.15, 308.15
Chen and Tu	2005	288.15, 298.15, 308.15
Ku and Tu	2005	298.15, 308.15, 318.15
Wang et al.	2005	298.15, 308.15, 318.15
Kretschmer et al.	1948	273.15, 298.15, 323.15

the basis for the following discussion of the temperature and composition dependence of the measured densities of the two binary systems.

4.4. Discussion of density–temperature dependencies of the mixtures

The majority of experimental literature data for properties of mixtures is limited to a narrow temperature range near ambient from approximately 280 K to 330 K. The densimeter used in this work has a temperature range of 270 K to 470 K. Figs. 8 and 9 show the densities of the two binary systems as a function of temperature. The data measured in this work at three compositions of each system are compared to the densities of the pure fluids at corresponding temperatures and at pressures of 3 MPa and 50 MPa, respectively. The densities of ethanol [11] and iso-octane [22] were calculated with the fundamental equations of state as implemented in NIST software REFPROP version 9.0 [21], while the densities of 2-butanol were measured previously in this instrument [7].

The graphs show that the density isobars of the non-polar iso-octane have weaker temperature dependence than any of the alcohol containing mixtures or the pure alcohols in the range of our measurements. At 3 MPa, the isobars of the mixtures containing 25.1% and

50% ethanol (Fig. 8) are close to the isobar of iso-octane but their temperature dependence is already pronouncedly stronger. The strongest temperature dependence is seen in the 3 MPa-isobar of pure ethanol. Note that at 430 K and above some densities of the ethanol-mixtures are lower than those of iso-octane. In the system of 2-butanol + iso-octane (Fig. 9), all densities of the mixtures are higher than those of iso-octane.

The picture changes significantly at the pressure of 50 MPa. The isobars at this pressure exhibit lower temperature dependencies and smaller variations from the non-polar iso-octane to the alcohols. At the highest measured temperature of 470 K, the densities of the mixtures containing 25.1% and 50% ethanol are very close or equal to that of iso-octane. In the system of 2-butanol + iso-octane (Fig. 9), only the density of the mixture with 25.1% 2-butanol appears to be close to that of iso-octane whereas that of the mixture with 50% 2-butanol is distinctly higher.

4.5. Discussion of density–mole fraction dependencies of the mixtures

Figs. 10 and 11 show the densities of the two binary systems vs. mole fraction of the respective alcohol, ethanol and 2-butanol. The varying influence of temperature on the densities of the mixtures and the pure fluids can also be seen because in each binary system, the isotherms at 270 K and 470 K are shown at 3 MPa and 50 MPa pressure. Conventionally, the composition dependence of mixture properties is examined in terms of the excess property which is the deviation of the volume of the mixture from the mole fraction average of the volumes of the mixture constituents at the same temperature and pressure. Figs. 10 and 11 illustrate that the excess densities for all compositions measured in the ranges of this work are negative.

Consideration of the excess densities only would miss the remarkable non-ideal characteristics that are apparent in the density diagrams of Figs. 10 and 11. While the densities at 270 K increase at both pressures steadily from those of iso-octane to those of the alcohols, significantly
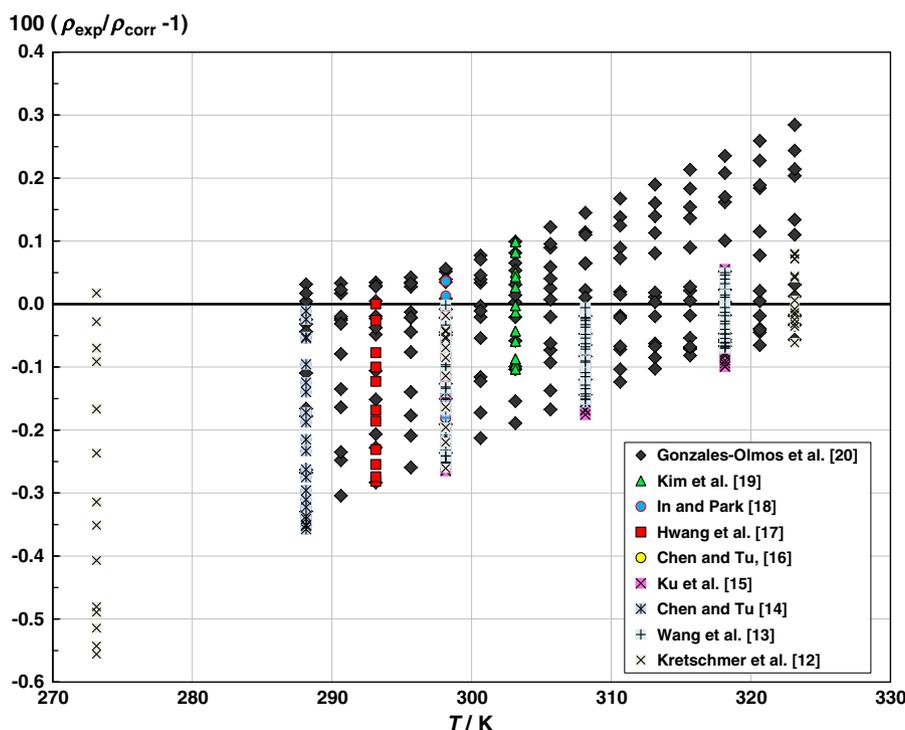
Fig. 4. Deviations of density data in the literature for the system ethanol + iso-octane (see Table 7) from values calculated with the preliminary Helmholtz free energy mixture model as a function of temperature at ambient pressure.
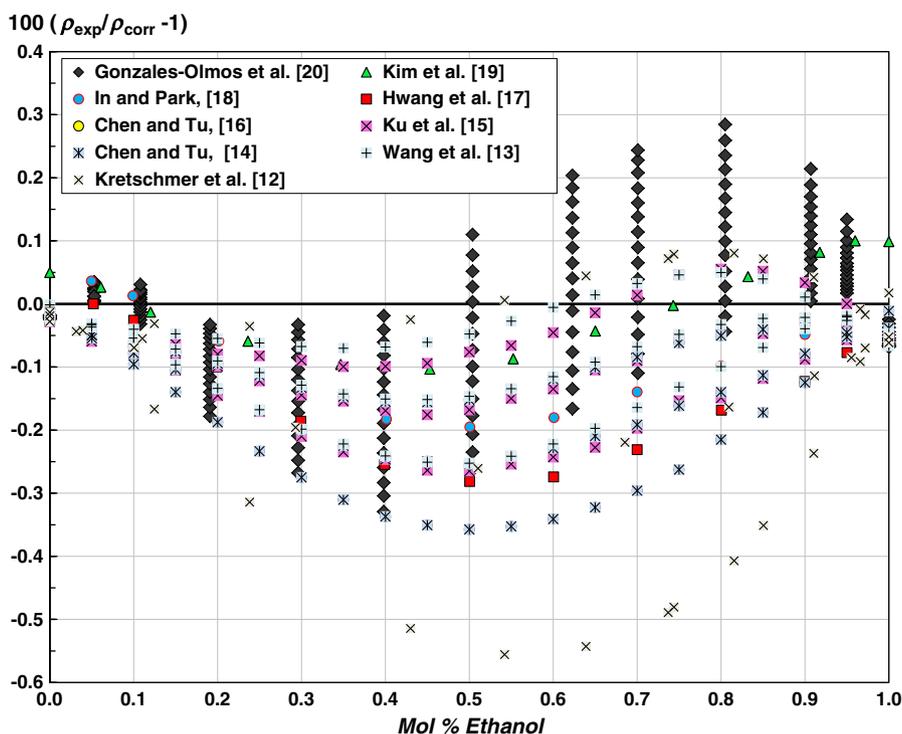
Fig. 5. Deviations of density data in the literature for the system ethanol + iso-octane (see Table 7) from values calculated with the preliminary Helmholtz free energy mixture model as a function of mole fraction of ethanol at ambient pressure.

different composition dependencies emerge at 470 K. Fig. 10 shows that the density of the system ethanol + iso-octane at 3 MPa pressure exhibits a distinct minimum at an ethanol mole fraction of 50% and only then begins to increase to the density of pure ethanol. Recall that the deviations between the present experimental data for the system ethanol + iso-octane and the preliminary Helmholtz mixture model were greatest at that composition and the temperatures 450 K and 470 K, cf. Fig. 2. Likewise, the deviations between literature data at atmospheric pressure and the preliminary Helmholtz mixture model for the system ethanol + iso-

octane were greatest in this range of compositions, cf. Fig. 5. This density minimum disappears when the pressure is increased to 50 MPa, but the density of the mixture remains close to that of iso-octane up to a mole fraction of ethanol of approximately 40%.

Fig. 11 shows that no density minimum occurs in the system 2-butanol + iso-octane in the range considered. Here, the composition dependence at the high end of the temperature range of the measurements is illustrated with two isotherms, that at 450 K and the partial isotherm at 470 K. At the lower pressure of 3 MPa and 450 K, the density remains relatively constant up to a mole fraction of 2-butanol of 25.1% and begins then to increase to that of pure 2-butanol. At the pressure of 50 MPa, the densities of the mixtures increase from that of iso-octane to that of 2-butanol at all isotherms shown.

5. Concluding remarks

With this work, we have expanded the scope of our densimetry of compressed liquids to binary mixtures and the composition dependence of their densities. Two systems of the nonpolar iso-octane with the highly polar ethanol and 2-butanol were selected because of their technical significance as model blends for the biofuel industry and because of their scientific relevance as little or not studied non-ideal mixtures whose properties are difficult to predict accurately. The measurement results at three compositions each of the two binary systems provide unique insights because of their wide temperature range from 270 K to 470 K with pressures to 50 MPa. Measurements over wide temperature ranges are particularly valuable for polar compounds and for mixtures of a polar and a non-polar compound.

The most notable feature of the densities measured in this work is the change of the density-composition dependence from low to high temperatures and at low pressures with the emergence of a density minimum in the equimolar mixture ethanol + iso-octane at 470 K. A preliminary Helmholtz free energy model was adjusted to the data for this binary system including an excess function adopted ad hoc

Fig. 6. Vapor pressures of ethanol, 2-butanol, and iso-octane as a function of temperature. The pressures were calculated with the correlations implemented in REFPROP [21] (ethanol and iso-octane) and DIPPR [23] (2-butanol). Ethanol and iso-octane have the same vapor pressure at 280 K while 2-butanol and iso-octane have the same vapor pressure at 375 K.
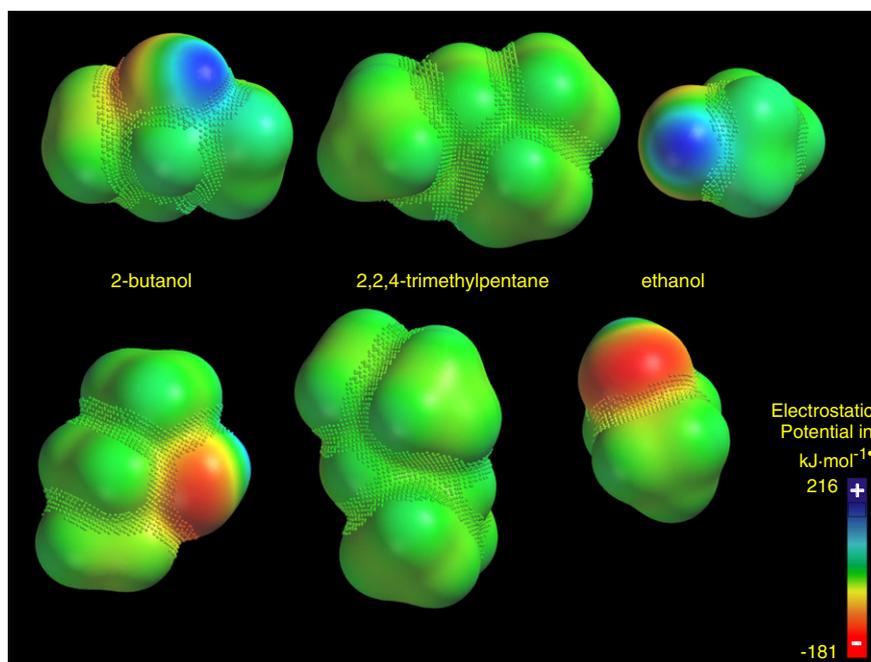
Fig. 7. Molecular size, shape, and charge distribution of the constituents of the mixtures measured in this work. All three molecules are shown on the same color scale for the electrostatic potential range of ethanol. Dots indicate those parts of the surfaces that are inaccessible for other molecules of the same species. Charge distributions of these molecules were calculated from first principles with the hybrid density functional model B3LYP and 6-311 + G** polarization basis sets.

Table 8
Calculated molecular characteristics of the mixture constituents. The geometrical properties relate to the isoelectron density surface at 0.002 electrons a.u.$^{-3}$.

Property	Unit	Ethanol	2-Butanol	2,2,4-Trimethylpentane
Volume	$(nm)^3$	0.06274	0.1022	0.1709
Surface area	$(nm)^2$	0.8410	0.1218	0.1784
Accessible surface area	$(nm)^2$	0.6738	0.8771	0.1197
Ovality	–	1.18	1.31	1.46
Polar surface area	$(nm)^2$	0.1581	0.1420	–
Dipole moment (calculated)	D	1.76	1.68	0.11
Dipole moment (experimental, evaluated, DIPPR [Rowley et al. [23]])	D	1.691	1.661	0

from a mixture of two polar fluorinated hydrocarbons. Comparisons between measured and calculated values show that accurate representation of the density minimum requires further refinement of the Helmholtz free energy model. The wide ranging experimental data measured in this work provide a foundation to develop an appropriate excess function for a highly non-ideal system that may be transferrable to other systems of similar or less pronounced non-ideality. For instance, once a model has been developed for the density of the system ethanol + iso-octane, it might be feasible to transfer to the density of the second system that was measured in this work, 2-butanol + iso-octane.

Acknowledgments
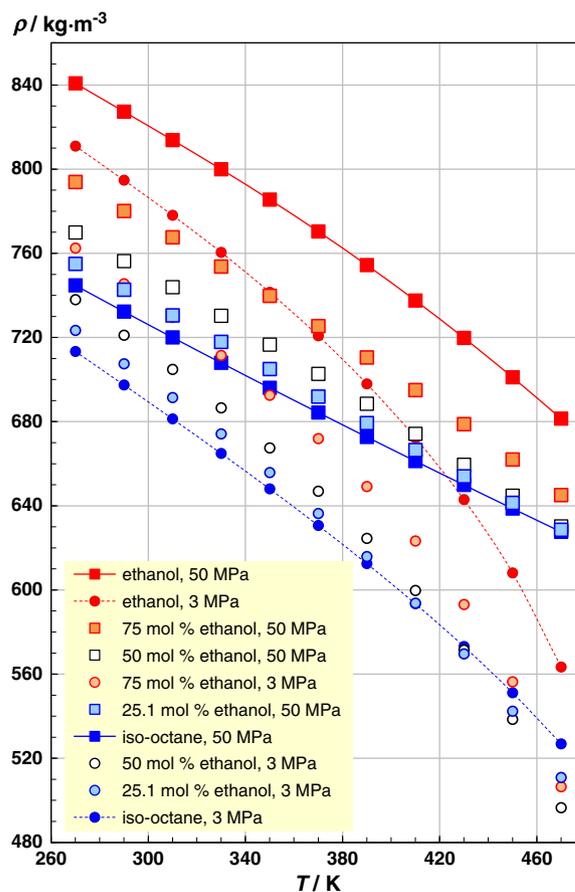
Fig. 8. Density isobars at 50 MPa and 3 MPa of the pure compounds and of three compositions of the system ethanol + iso-octane as a function of temperature. Lines are drawn to guide the eye of the reader.
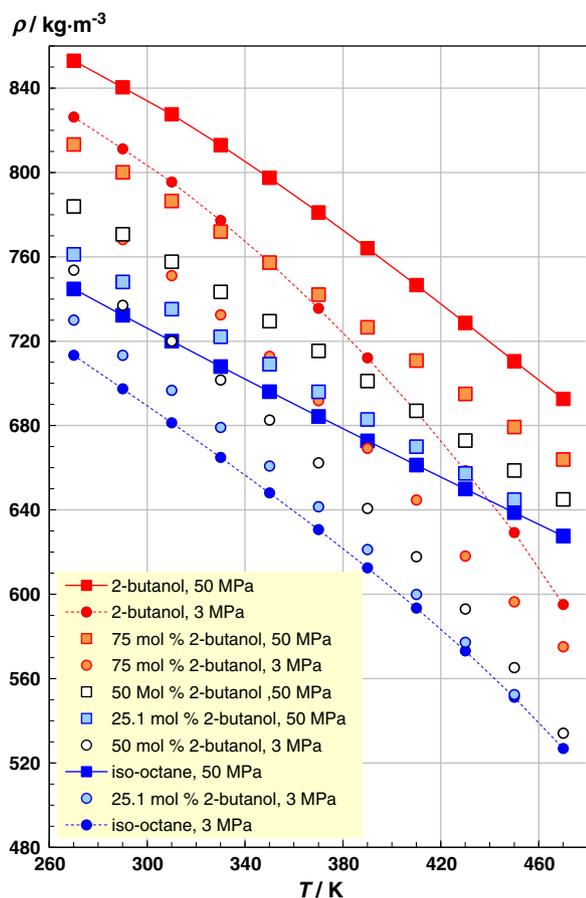
Fig. 9. Density isobars at 50 MPa and 3 MPa of the pure compounds and of three compositions of the system 2-butanol + iso-octane as a function of temperature. Lines are drawn to guide the eye of the reader.

Fig. 10. Density isotherms at 50 MPa and 3 MPa and at two temperatures of the system ethanol + iso-octane as a function of mixture composition. Lines are drawn to guide the eye of the reader.

References

[1] 1988–1989 Oxygenated Fuels Program, Air Pollution Control Division Final Report to the Colorado Air Quality Control Commission, Colorado Dept. of Health, Denver, Colorado, USA, 1989.
[2] S.L. Outcalt, M.O. McLinden, Industrial and Engineering Chemistry Research 46 (2007) 8264–8269.
[3] T.J. Bruno, A. Laesecke, S.L. Outcalt, H.D. Seelig, B.L. Smith, NISTIR 6647, 2007. 32 pp.
[4] A. Laesecke, S.L. Outcalt, K.J. Brumback, Energy & Fuels 22 (2008) 2629–2636.
[5] S. Outcalt, A. Laesecke, M.B. Freund, Energy & Fuels 23 (2009) 1626–1633.
[6] S.L. Outcalt, A. Laesecke, K.J. Brumback, Journal of Propulsion and Power 25 (2009) 1032–1040.
[7] S.L. Outcalt, A. Laesecke, T.J. Fortin, Journal of Molecular Liquids 151 (2010) 50–59.
[8] S.L. Outcalt, Journal of Chemical and Engineering Data 56 (2011) 4239–4243.
[9] S.L. Outcalt, T.J. Fortin, Journal of Chemical and Engineering Data 56 (2011) 3201–3207.
[10] E.W. Lemmon, R.T. Jacobsen, Journal of Physical and Chemical Reference Data 33 (2004) 593–620.
[11] J.A. Schroeder, A New Fundamental Equation for Ethanol, University of Idaho, 2011.
[12] C.B. Kretschmer, J. Nowakowska, R. Wiebe, Journal of the American Chemical Society 5 (1948) 1785–1790.
[13] C.C. Wang, H.W. Chen, C.H. Tu, Journal of Chemical and Engineering Data 50 (2005) 1687–1693.
[14] H.W. Chen, C.H. Tu, Journal of Chemical and Engineering Data 50 (2005) 1262–1269.
[15] H.C. Ku, C.H. Tu, Journal of Chemical and Engineering Data 50 (2005) 608–615.
[16] H.W. Chen, C.H. Tu, Journal of Chemical and Engineering Data 51 (2006) 261–267.
[17] I.C. Hwang, H.M. Lim, S.J. Park, K.J. Han, I.H. Park, Fluid Phase Equilibria 259 (2007) 146–152.
[18] S.J. In, S.J. Park, Industrial and Engineering Chemistry Research 14 (2008) 377–381.
[19] H.D. Kim, I.C. Hwang, S.J. Park, Journal of Chemical and Engineering Data 54 (2009) 3051–3058.
[20] R. Gonzalez-Olmos, M. Iglesias, S. Mattedi, Physics and Chemistry of Liquids 48 (2010) 337–384.
[21] E.W. Lemmon, M.L. Huber, M.O. McLinden, http://www.nist.gov/srd/nist23.htm 2010.
[22] E.W. Lemmon, Equation of State for the Thermodynamic Properties of 2,2,4-trimethylpentane, 2012, private communication.
[23] R.L. Rowley, W.V. Wilding, J.L. Oscarson, http://aiche.org/dippr/ 2007.
[24] T.A. Litovitz, The Journal of Chemical Physics 20 (1952) 245–256.
[25] P. Debye, Polar Molecules, The Chemical Catalog Comp., Inc., 1929. 172 pp.
[26] C.P. Smyth, In: in: L.P. Hammett (Ed.), International Chemical Series, McGraw-Hill, Inc., New York, NY, 1955, 441 pp.
[27] E. Arunan, G.R. Desiraju, R.A. Klein, J. Sadlej, S. Scheiner, I. Alkorta, D.C. Clary, R.H. Crabtree, J.J. Dannenberg, P. Hobza, H.G. Kjaergaard, A.C. Legon, B. Mennucci, D.J. Nesbitt, Pure and Applied Chemistry 83 (2011) 1619–1636.
[28] E. Arunan, G.R. Desiraju, R.A. Klein, J. Sadlej, S. Scheiner, I. Alkorta, D.C. Clary, R.H. Crabtree, J.J. Dannenberg, P. Hobza, H.G. Kjaergaard, A.C. Legon, B. Mennucci, D.J. Nesbitt, Pure and Applied Chemistry 83 (2011) 1637–1641.
[29] W.J. Hehre, A Guide to Molecular Mechanics and Quantum Chemical Calculations, Wavefunction, Inc., Irvine, CA, 2003. 796 pp.
[30] P. Ertl, In: in: R. Mannhold, et al., (Eds.), Molecular Drug Properties, Wiley-VCH, 2007, pp. 111–126.
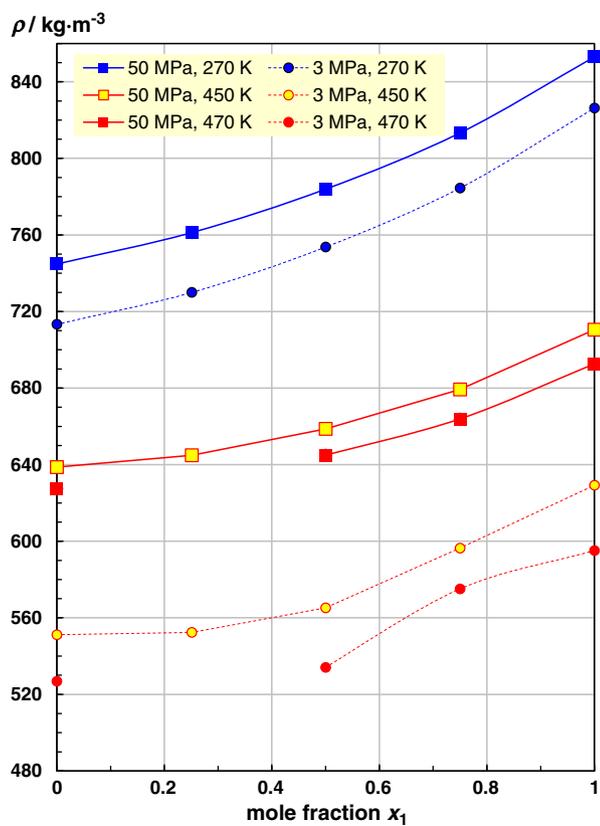
Fig. 11. Density isotherms of the system 2-butanol + iso-octane at 50 MPa and 3 MPa and at three temperatures as a function of mixture composition. Lines are drawn to guide the eye of the reader.